JOURNAL OF MATERIALS SCIENCE 15 (1980) 2066–2072

# The relationship between the a.c. impedance and microstructure of a sodium β-alumina ceramic

W. I. ARCHER, R. D. ARMSTRONG, D. P. SELLICK
*Electrochemistry Research Laboratories, School of Chemistry, University of Newcastle upon Tyne, UK*

W. G. BUGDEN, J. H. DUNCAN
*Research and Development Division, British Railways Board, London Road, Derby, UK*

A comparison is made between the microstructures, resistivities and strengths of sodium $\beta/\beta''$-alumina samples prepared under different firing conditions. Double peak firing schedules are shown to result in samples of higher strength with a narrower grain-size distribution and lower resistivity than those produced by single peak firing. Complex plane a.c. impedance and admittance data show the sodium ion conduction over the temperature range 173 to 300 K to be governed primarily by intergranular regions of the sample (with the resistance varying with grain size) whilst resistivity measurements at 623 K show the conduction to be primarily intragranular controlled at elevated temperatures.

## 1. Introduction

The use of polycrystalline sodium $\beta/\beta''$-alumina in the sodium/sulphur cell is well known. For this use a ceramic of high strength and low resistance at high temperatures is required and a large amount of time has been spent in developing manufacturing techniques to fulfil these requirements. The single peak firing schedules used in the sintering of β-alumina may easily result in samples having a duplex microstructure and, therefore, reduced strength. Although minimizing both the sintering time and temperature reduces the grain-size distribution of a sample, the fired density and phase conversion of β-alumina to the lower resistivity $\beta''$-alumina are also reduced. In a recent paper by Bugden and Duncan [1] attention was brought to a double peak firing schedule (Fig. 1) which greatly restricts the growth of a duplex microstructure while maintaining or improving properties such as $\beta''$-alumina conversion and strength.

Complex plane a.c. impedance and admittance techniques have been used in a number of studies on polycrystalline sodium $\beta/\beta''$-alumina [2 – 7]. The theory of the use of the technique has been discussed by Armstrong *et al.* [2] and only a brief account will be given here. Fig. 2a shows the equivalent circuit used to represent the polycrystalline ceramic in contact with sodium ion blocking electrodes (e.g. gold). In this circuit $C_g$ and $R_b$ represent the geometric (bulk) capacitance and bulk resistance of the grains, whilst $C_{gb}$ and $R_{gb}$ represent the capacitance and resistance of the grain-boundary regions. The blocking electrode/electrolyte interface gives rise to a double layer capacitance, $C_{dl}$. The theoretical complex plane a.c. impedance and admittance spectra derived from the equivalent circuit are shown in Fig. 2b and c, respectively (N.B. only when the majority of the surface roughness is removed from the ceramic by polishing will the capacitance line arising from $C_{dl}$ in the impedance spectrum be close to vertical [8]; poor surface preparation can also be shown to have a detrimental effect on complex plane admittance spectra). Complex plane spectra, therefore, allow the individual resistances $R_T$ (total resistance), $R_{gb}$ and $R_b$ to be derived.

In this paper a comparison is made between the microstructures, high-temperature resistivity and strength of two samples prepared by a double peak firing routine (no. 2 in Fig. 1) and a sample pre-


0022–2461/80/082066–07$02.70/0 © *1980 Chapman and Hall Ltd.*

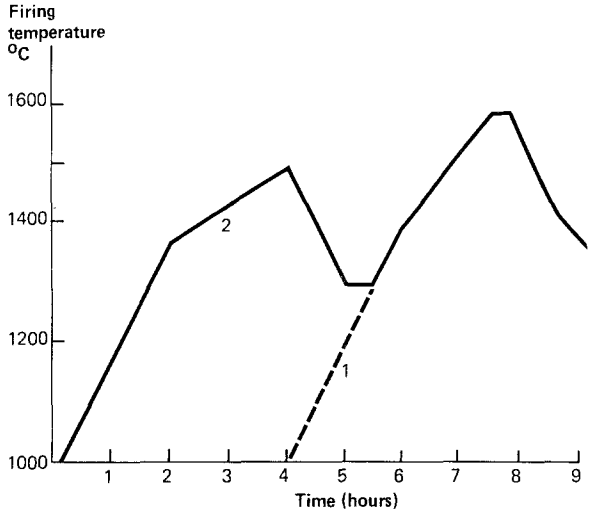


*Figure 1* Firing schedule for single peak (1) and double peak (2) firings.

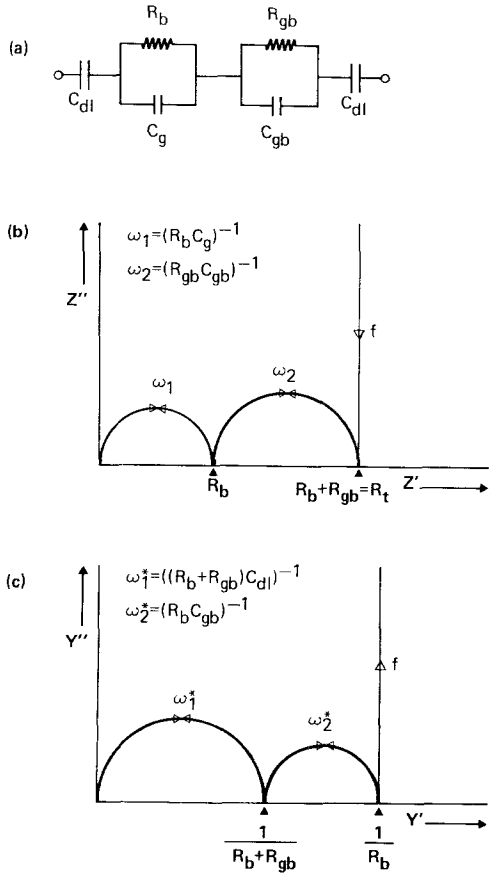


*Figure 2* (a) Equivalent circuit for polycrystalline sodium $\beta/\beta''$-alumina with blocking electrodes. $C_{dl}$ = double layer capacitance of electrode/electrolyte interface. $R_b$ = intragranular (bulk) resistance. $C_g$ = geometric (bulk) capacitance. $R_{gb}$ and $C_{gb}$ = grain-boundary resistance and capacitance. (b) Theoretical complex plane impedance spectrum arising from (a). (c) Theoretical complex plane admittance spectrum arising from (a).

pared by a single peak firing schedule (no. 1 in Fig. 1). A sample prepared by a single peak firing technique with a hold time incorporated in the heating up time has also been studied. A correlation between the microstructures of the samples and complex plane data for the temperature range 173 to 300 K has been attempted.

## 2. Experimental procedure

Sodium $\beta$-alumina tubes (33 mm diameter and 200 mm long) of composition 90.4 wt% $Al_2O_3$, 8.9 wt% $Na_2O$ and 0.7 wt% $Li_2O$, were isostatically pressed at 240 MN m$^{-2}$ from spray-dried powder and fired in an electric kiln to a top temperature of approximately 1600° C. A ramp generator was used to control the rate of temperature rise over the final 200° C of the firing. The top temperature was controlled by a digital set-point instrument with a 1 $\mu$V adjustment connected to a calibrated 6/30 Rh/Pt thermocouple to give a reproducibility of ± 1° C. The time at the top temperature was electronically controlled. Temperature gradients within the kiln were minimized by adjusting the power to separate groups of elements.

The tubes were fired in crucibles of high thermal capacity (to reduce property differences along their length) according to the schedules shown in Table I. Also shown in Table I are the strengths (± 5%) and densities (± 0.3%) for the samples as a result of the differing firing techniques. The physical properties of the ceramics were found to be reproducible in duplicate firings. The $\beta''$-alumina content of the samples was determined by X-ray diffraction to be > 90%.

TABLE I The firing condition, strength and density of the four sodium $\beta/\beta''$-alumina samples

| | Firing conditions | Strength ($MN\,m^{-2}$) | Density ($kg\,m^{-3}$) |
|---|---|---|---|
| Sample 1 | Double peak firing. Top temperature of 1607° C for 15 min | 190 | 3220 |
| Sample 2 | Double peak firing. Top temperature of 1612° C for 15 min | 212 | 3230 |
| Sample 3 | Single peak firing to 1607° C for 15 min | 153 | 3220 |
| Sample 4 | Single peak firing with hold at 1540° C for 2 h then raised to a top temperature of 1612° C (for 15 min) without cooling | 67 | 3200 |

Complex plane impedance measurements were carried out on the cell: Au/Na$\beta/\beta''$-Alumina/Au. Annulet samples (approximately 6 mm long) were cut from the tubes and the flat faces polished with successive grades of diamond lapping compound down to 1 $\mu$m. After washing in the minimum quantity of ethanol, the samples were baked out in a furnace at 800° C for 4 h, then stored in an oven at 230° C until used. Gold electrodes were applied to the polished surfaces using a Polaron SEM sputter coater. Stainless steel plates were used as electrical contacts in the cell assembly. The sample preparation technique and cell assembly are described more fully by Armstrong and Sellick [7].

Impedance measurements were carried out over a frequency range of $10^{-1}$ to $10^{6}$ Hz using a Solartron 1174 Frequency Response Analyser. The use of such a system has been covered in greater detail elsewhere [9, 10].

Complex plane impedance data were obtained over a temperature range of 173 to 300 K. All measurements were made with the cell under a stream of dry nitrogen. Cooling of the sample was carried out by passing the stream of nitrogen over liquid nitrogen prior to reaching the cell. The temperature was monitored by a thermocouple attached to the side of the cell. Complex plane admittance data were calculated from the experimental impedance data.

The resistivity of the samples at 623 K was measured using an a.c. technique at a frequency of 20 kHz with reversible electrodes of molten sodium nitrate. The sample size and preparation was similar to that for the a.c. impedance studies. Temperature cycling from 593 to 653 K was carried out to check the reversibility of the system.

Microstructural studies were made on samples which had been polished down to 1 $\mu$m and thermally etched at 1500° C in air for 15 min. Optical micrographs were obtained using a Zeiss Ultraphot instrument.

## 3. Results and discussion

### 3.1. The ceramic microstructures

Optical micrographs for samples 1 to 4 are shown in Figs. 3a to d, respectively. The double peak firing schedule to a top temperature of 1607° C given to sample 1 results in the suppression of grain growth beyond about 40 $\mu$m. The additional thermal energy input resulting from the double peak firing, however, causes growth of the smallest grains to give a high proportion in the size range 2 to 4 $\mu$m.

In sample 2, also a double peak firing, the top temperature was raised to 1612° C. The effect of this is to increase further the size of the small grains in the matrix while the larger grains remain little altered.

Sample 3 demonstrates the duplex grain structure found with firing schedules having a single peak; in this case to 1607° C. Grains up to 175 $\mu$m long are visible in the microstructure although the fine-grained matrix contains a higher proportion of grains below 2 $\mu$m. The microstructure of sample 3 (Fig. 3c) contrasts greatly with that of sample 1 (Fig. 3a) which results from a double peak schedule to the same top temperature.

The 2 h hold at 1540° C for sample 4 allows a considerable amount of sintering to occur. On the model proposed by Bugden and Duncan [1] this would be accompanied by grain growth of the original three-block $\beta''$-alumina nuclei, which have to be shown to grow in an exaggerated manner compared with the two-block $\beta$-alumina [11] and accounts for the large number of grains up to 240 $\mu$m visible in the final microstructure. After the 2 h hold, the temperature was raised to 1612° C without a cooldown. This firing schedule can, therefore, be contrasted with the double peak firing of sample 2 where the maximum grain size is only about 40 $\mu$m (Fig. 3b). Many more of the smallest grains in sample 4, however, are seen to be below 2 $\mu$m.

It may be observed from the values in Table I that the density and strength of the resultant sodium $\beta/\beta''$-alumina sample is increased by both the double peak firing technique and by raising the

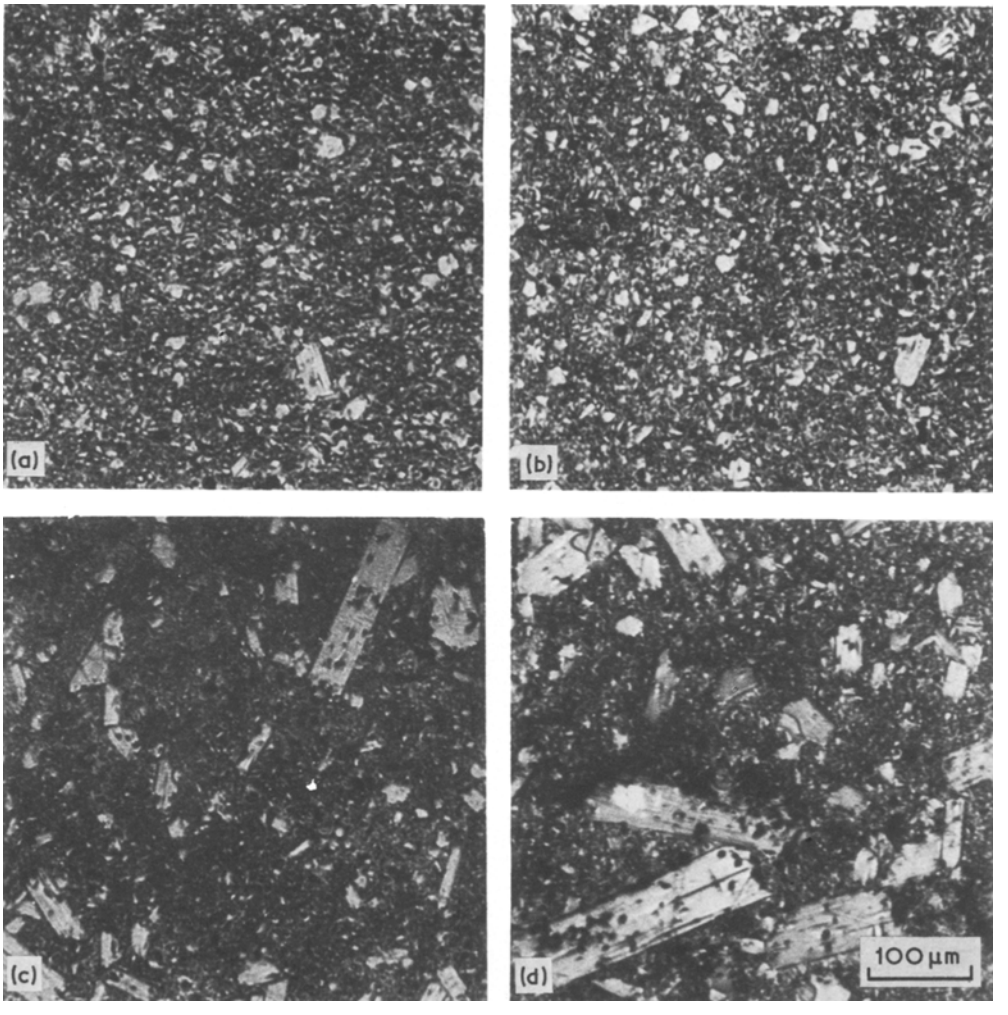


*Figure 3* Optical micrographs of (a) sample 1, (b) sample 2, (c) sample 3, and (d) sample 4.

top temperature of the firing. Although when contrasted with sample 1, sample 2 has the slightly coarser microstructure due to the higher firing temperature, the slightly greater density (and therefore reduced porosity) results in sample 2 having the greater strength (Table I). In sample 4, the hold at 1540° C results in exaggerated grain growth thereby reducing the strength of the sample.

## 3.2. Electrical resistivity measurements

### *3.2.1. High-temperature resistivity data*

Resistivity data (± 0.05 Ω cm) for samples 1 to 4 at 623 K are shown in Table II. The values obtained are consistent with both the different firing schedules which the four samples had been subjected to and the resulting microstructures.

Samples 1 and 2, fired to a double peak sched-

TABLE II Resistivity values and activation energies for the four sodium $\beta/\beta''$-alumina samples. $R_T$ = total resistivity, $R_{gb}$ = intergranular resistivity and $R_b$ = bulk (intragranular) resistivity

| | Total resistivity at 623 K (Ω cm) | Resistivity at 223 K (kΩ cm) | | | Resistivity at 298 K (kΩ cm) | | | Activation energies (kJ mol$^{-1}$) | | |
|---|---|---|---|---|---|---|---|---|---|---|
| | | $R_T$ | $R_{gb}$ | $R_b$ | $R_T$ | $R_{gb}$ | $R_b$ | $R_T$ | $R_{gb}$ | $R_b$ |
| Sample 1 | 2.93 | 40.24 | 33.38 | 6.86 | 0.92 | 0.75 | 0.17 | 28.0 | 28.0 | 26.5 |
| Sample 2 | 3.00 | 56.96 | 50.03 | 6.93 | 1.20 | 1.03 | 0.17 | 28.5 | 28.5 | 27.0 |
| Sample 3 | 3.26 | 21.50 | 17.00 | 4.50 | 0.58 | 0.44 | 0.14 | 27.0 | 27.0 | 26.0 |
| Sample 4 | 2.18 | 20.76 | 16.72 | 4.04 | 0.50 | 0.36 | 0.14 | 27.5 | 28.0 | 24.0 |

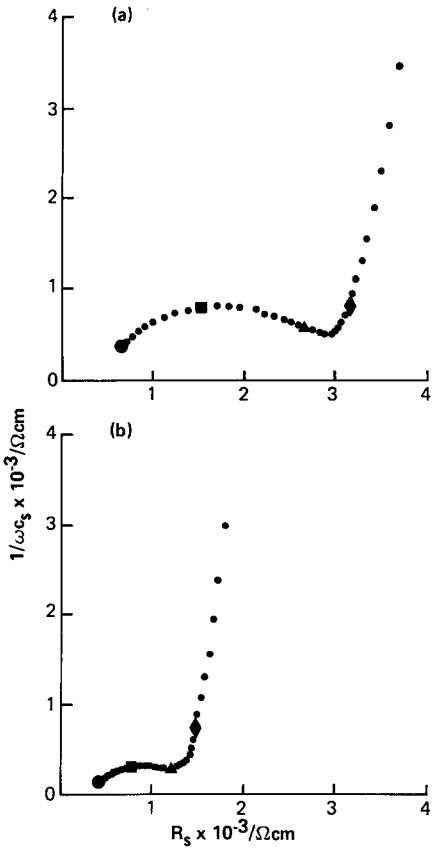


*Figure 4* Complex plane impedance spectra of (a) sample 2 and (b) sample 3 at 273 K. • 1 MHz, ▪ 125 kHz, ▲ 12.5 kHz, ◆ 1.25 kHz.

ule, are observed to have a lower resistivity than sample 3, derived from a single peak firing. This can be attributed to the fact that although the maximum grain size is larger in sample 3 than in samples 1 and 2, the matrix grains are considerably finer than for the double peak firings where the increased heatwork input causes extra growth of the matrix grains. For sample 4 the hold at 1540° C has resulted in further growth of the larger (predominantly $\beta''$-alumina) grains and the contribution to the resistivity by the fine-grained matrix is less. Hence the electrical resistivity of sample 4 is somewhat less than that of the other samples.

It may be deduced from these results that the sodium ion conduction at 623 K is primarily controlled by the intragranular regions of the electrolyte. However, it is apparent that a finite proportion of the conduction is derived from the intergranular regions at elevated temperatures, as a comparison between the resistivities of samples 1 and 2 shows that of sample 1 to be slightly lower than the resistivity of sample 2, even though sample 2 was fired to the higher temperature.

### 3.2.2. Low-temperature complex plane resistivity data

A comparison between the complex plane impedance spectra of samples 2 (relatively fine grain) and 3 (with a higher proportion of coarser grains) is shown in Figs. 4a and b. It may be observed that the spectrum derived from sample 3 (at 273 K) shows an intergranular component smaller than that of sample 2. (It should be noted that the temperature at which these spectra were measured was too high to show the bulk semicircle.) The same trend was noticed for all four samples; the greater the number of coarser grains, the smaller the intergranular semi-circle. The corresponding complex plane admittance spectra are shown in Figs. 5a and b.

The total, intergranular and bulk resistivities for each sample were obtained by extrapolation of the relevant components of the impedance and admittance spectra, as shown in Fig. 2. The total resistance was primarily derived from the impedance spectra as extrapolation of a straight line was thought to be more accurate than that of a semicircle. The values obtained from the two methods were found to be in very good agreement with each other (better than 10%). This serves as a suitable method for cross-checking the results as the features in both spectra arise from the combination of different parameter (Fig. 2).

Resistivity data (± 5%) derived from the complex plane techniques for the four samples at 223 and 298 K are shown in Table II.

Arrhenius plots of log $R_T$, log $R_{gb}$ and log $R_b$ versus $1/T$, as shown in Fig. 6 (for sample 1) were linear over the temperature range studied. Activation energies derived from such plots are also shown in Table II. There was found to be no great variation in the activation energies derived for $R_T$, $R_{gb}$ and $R_b$ throughout the four samples.

A study of the total and intergranular resistivities in Table II reveals the trend that the greater the number of coarse grains, the lower the resistivity of the sample. This suggests that at low temperatures the sodium ion conduction is primarily controlled by the intergranular regions of the electrolyte with the intergranular area being the controlling factor. This contrasts with the intragranular control at high temperatures discussed earlier. Although the microstructure of sample 2 is slightly coarser than that of sample 1, its resis-

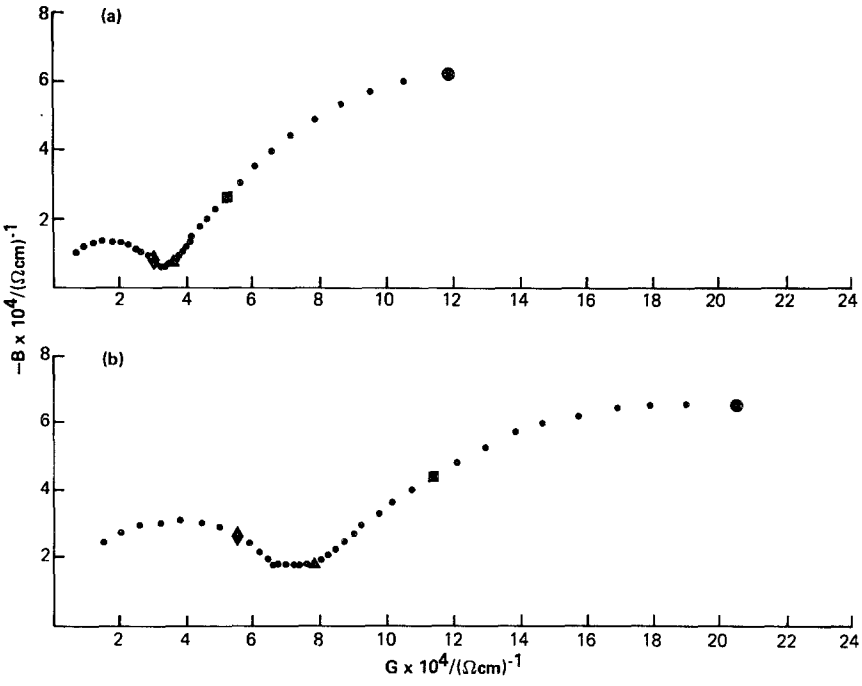


*Figure 5* Complex plane admittance spectra of (a) sample 2 and (b) sample 3 at 273 K. • 1 MHz, ▪ 125 kHz, ▲ 12.5 kHz ♦ 1.25 kHz.

tivity is higher. We attribute this to the greater porosity of sample 1.

The bulk resistivity values shown in Table II are considerably lower than those for the total and intergranular resistivities and may be regarded as having a higher error attached to them. However, it does appear that the $R_b$ values for samples 3 and 4 are consistently lower than those for samples 1 and 2. This may be a result of the coarser grains within these samples.

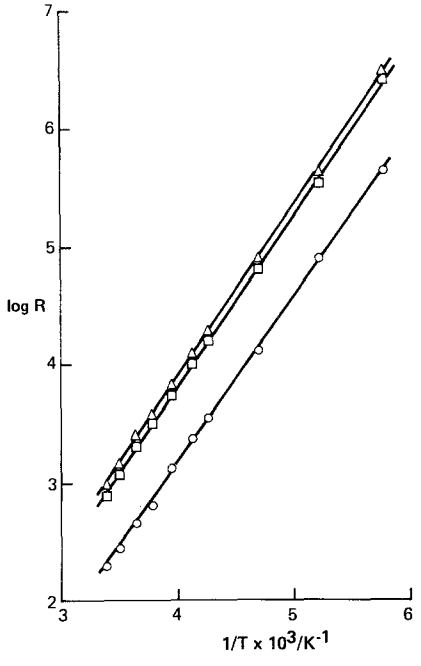


*Figure 6* Arrhenius plots for sample 1. △ Total resistivity, □ intergranular resistivity, ○ intragranular (bulk) resistivity.

A noticeable feature in the data derived from the complex plane technique at low temperatures is the rather high values obtained for the intragranular (bulk) activation energies; 26 kJ $mol^{-1}$ as opposed to 16 kJ $mol^{-1}$ for single crystal sodium $\beta$-alumina [12]. Although this feature could arise from the presence of water, the authors feel confident that sufficient precautions were taken to eliminate this possibility; the reproducibility of this feature throughout different samples also reduces the probability of the presence of water. In order for the low-temperature intragranular data to correlate with the high-temperature resistivity data and with activation energies for conduction at higher temperatures closer to those of single crystal material, some curvature in the Arrhenius plot must be experienced. For this reason, therefore, the authors believe that the high activation energies obtained for intragranular conduction arise from tortuosity factors (which are temperature-dependent) similar to those proposed by Grant *et al.* [13] and Powers and Mitoff [14].

## 4. Conclusions

In this paper we have shown the distinct advantages of a double peak firing schedule (no. 2 in Fig. 1) over that of a single peak firing schedule (no. 1 in Fig. 1). Ceramic samples derived from the former firing schedule were found to have high strength and density with a narrow grain-size distribution and low resistivity at high temperature. This may be contrasted with the highly duplex microstructure and greater resistivity of samples obtained using a single peak firing schedule. It is believed that the benefits derived from the double peak firing schedule are due to an increase in the number of three-block ($\beta''$) alumina nuclei during the cooldown and reheat stages when sintering is suppressed. When sintering recommences, the increased number of $\beta''$ nuclei grow competitively and none can grow to sizes beyond about 40 $\mu$m. A sample held at 1540° C for 2 h before raising to a top temperature of 1610° C without a cooldown resulted in a microstructure showing exaggerated grain growth. The sample was of low strength but had a resistivity at high temperature lower than that of the other samples. This can be explained by assuming that the largest grains are entirely three-block ($\beta''$) alumina structure [15].

Resistivity data at high temperature (623 K) shows the sodium ion conduction to be controlled primarily by the intragranular (bulk) regions of the sample and are consistent with the firing schedules for each sample. Complex plane impedance measurements at temperatures lower than 300 K, however, show intergranular-controlled conduction with resistivity varying with grain size. This has been attributed to the variation in the area of the grain-boundary region for the different samples. It is believed that high activation energies for intragranular conduction at low temperatures are the result of the more direct conduction path through mis-orientated crystals in the polycrystalline material as opposed to the more tortuous, but preferred, conduction path at high temperatures.


## Acknowledgements

W. I. Archer, R. D. Armstrong and D. P. Sellick are grateful to the Science Research Council for supporting this work. W. G. Bugden and J. H. Duncan wish to thank the British Railways Board for permission to publish this paper and the Department of Transport for funding the work at British Rail.


## References


1. W. G. BUGDEN and J. H. DUNCAN, Second International Meeting on Solid Electrolytes, Paper 4.4, St Andrews, Scotland, September (1978).
2. R. D. ARMSTRONG, T. DICKINSON and P. M. WILLIS, *J. Electroanal. Chem.* **53** (1974) 389.
3. R. W. POWERS and S. P. MITOFF, *J. Electrochem. Soc.* **122** (1975) 226.
4. I. M. HODGE, M. D. INGRAM and A. R. WEST, *J. Electroanal. Chem.* **74** (1976) 125.
5. L. C. DE JONGHE, *J. Mater. Sci.* **14** (1979) 33.
6. J. H. KENNEDY, J. R. AKRIDGE and M. KLEITZ, *Electrochim. Acta* **24** (1979).
7. R. D. ARMSTRONG and D. P. SELLICK, *J. Appl. Electrochem.* **9** (1979) 623.
8. R. D. ARMSTRONG and R. A. BURNHAM, *J. Electroanal. Chem.* **72** (1976) 257.
9. R. D. ARMSTRONG, M. F. BELL and A. A. METCALFE, *ibid.* **77** (1977) 287.
10. W. I. ARCHER and R. D. ARMSTRONG, "Specialist Periodical Reports – Electrochemistry", Vol. 7 (The Chemical Society, London, 1980).
11. J. FALLY, C. LASNE, Y. LAZENNEC, Y. LE CARS and P. MARGOTIN, *J. Electrochem. Soc.* **120** (1973) 1296.
12. M. S. WHITTINGHAM and R. A. HUGGINS, *J. Chem. Phys.* **54** (1971) 414.
13. R. J. GRANT, M. D. INGRAM and A. R. WEST, *Electrochim. Acta* **22** (1977) 729.
14. R. W. POWERS and S. P. MITOFF, "Solid Electrolytes – General Principles, Characterisation, Materials, Applications", edited by P. Hagenmuller and W. van Gool (Academic Press, New York and London, 1978) pp. 123–44.
15. J. W. HARDING and S. E. LARELL, private communication, British Rail, Derby.


Received 31 May 1979 and accepted 21 January 1980.